

# Treatment of CHO cells with Taxol and reversine improves micronucleation and microcell-mediated chromosome transfer efficiency

Narumi Uno,<sup>1,2,6</sup> Hiroyuki Satofuka,<sup>2,6</sup> Hitomaru Miyamoto,<sup>3,6</sup> Kazuhisa Honma,<sup>3</sup> Teruhiko Suzuki,<sup>4</sup> Kyotaro Yamazaki,<sup>3,5</sup> Ryota Ito,<sup>1</sup> Takashi Moriwaki,<sup>2,3</sup> Shusei Hamamichi,<sup>2</sup> Kazuma Tomizuka,<sup>1</sup> Mitsuo Oshimura,<sup>2</sup> and Yasuhiro Kazuki<sup>2,3,5</sup>

<sup>1</sup>Laboratory of Bioengineering, Faculty of Life Sciences, Tokyo University of Pharmacy and Life Sciences, 1432-1 Horinouchi, Hachioji, Tokyo 192-0392, Japan; <sup>2</sup>Chromosome Engineering Research Center, Tottori University, 86 Nishi-cho, Yonago, Tottori 683-8503, Japan; <sup>3</sup>Department of Chromosome Biomedical Engineering, School of Life Science, Faculty of Medicine, Tottori University, 86 Nishi-cho, Yonago, Tottori 683-8503, Japan; <sup>4</sup>Stem Cell Project, Tokyo Metropolitan Institute of Medical Science, Kamikitazawa, Setagaya-ku, Tokyo 156-8506, Japan; <sup>5</sup>Chromosome Engineering Research Group, The Exploratory Research Center on Life and Living Systems (ExCELLS), National Institutes of Natural Sciences, 5-1 Higashiyama, Myodaiji, Okazaki, Aichi 444-8787, Japan

**Microcell-mediated chromosome transfer is an attractive technique for transferring chromosomes from donor cells to recipient cells and has enabled the generation of cell lines and humanized animal models that contain megabase-sized gene(s). However, improvements in chromosomal transfer efficiency are still needed to accelerate the production of these cells and animals. The chromosomal transfer protocol consists of micronucleation, microcell formation, and fusion of donor cells with recipient cells. We found that the combination of Taxol (paclitaxel) and reversine rather than the conventional reagent colcemid resulted in highly efficient micronucleation and substantially improved chromosomal transfer efficiency from Chinese hamster ovary donor cells to HT1080 and NIH3T3 recipient cells by up to 18.3- and 4.9-fold, respectively. Furthermore, chromosome transfer efficiency to human induced pluripotent stem cells, which rarely occurred with colcemid, was also clearly improved after Taxol and reversine treatment. These results might be related to Taxol increasing the number of spindle poles, leading to multinucleation and delaying mitosis, and reversine inducing mitotic slippage and decreasing the duration of mitosis. Here, we demonstrated that an alternative optimized protocol improved chromosome transfer efficiency into various cell lines. These data advance chromosomal engineering technology and the use of human artificial chromosomes in genetic and regenerative medical research.**

## INTRODUCTION

Microcell-mediated chromosome transfer (MMCT) is a core technology that allows the introduction of megabase-sized DNA from donor cells to recipient cells.<sup>1</sup> MMCT can overcome the size limitation of conventional gene transfer methods that use viral or plasmid vectors.<sup>2-5</sup> Through this technology, we successfully generated novel cell lines for regenerative medicine research,<sup>6</sup> as well as humanized

animal models, including models for Down syndrome,<sup>7</sup> drug metabolism,<sup>8</sup> and production of human antibodies.<sup>9,10</sup> Thus, MMCT is a key technology for research and development using chromosomal engineering, and consequently, various improved protocols have been developed.<sup>11-16</sup>

The MMCT protocol consists of three steps: induction of micronucleation by mitotic spindle inhibitor(s), microcell formation by disrupting the actin cytoskeleton, and fusion of the resulting microcells with recipient cells.<sup>3</sup> Colcemid and colchicine, both microtubule polymerization inhibitors (microtubule destabilizers),<sup>17</sup> are conventional reagents used for the induction of micronucleation in Chinese hamster ovary (CHO) cells. The combination of TN-16 (microtubule destabilizer)<sup>18</sup> and griseofulvin (microtubule stabilizer)<sup>19</sup> was also shown to increase MMCT efficiency by 3.8-fold.<sup>14</sup> We previously reported that mitotic slippage without proper chromosome segregation is required for micronucleation.<sup>20</sup> A recent study showed that the combination of Taxol (paclitaxel) and reversine induced micronucleation in HeLa cells.<sup>21</sup> Although the conventional reagent colcemid is a microtubule destabilizer, Taxol is a microtubule stabilizer, and reversine is an inhibitor of the spindle assembly checkpoint (SAC) proteins, MPS1 protein kinase<sup>22</sup> and aurora kinases A, B, and C.<sup>23</sup> Therefore, micronucleation induction by microtubule stabilizing and mitotic slippage-inducing reagents may produce different chromosomal dynamics and packaging into micronuclei and, subsequently, improve MMCT efficiency.

Received 25 July 2022; accepted 11 July 2023;  
<https://doi.org/10.1016/j.omtn.2023.07.002>.

<sup>6</sup>These authors contributed equally

**Correspondence:** Yasuhiro Kazuki, Tottori University, 86 Nishi-cho, Yonago, Tottori 683-8503, Japan.

**E-mail:** [kazuki@tottori-u.ac.jp](mailto:kazuki@tottori-u.ac.jp)



In this study, we hypothesized that the combined use of Taxol and reversine (TR) would improve the rate of micronucleation in CHO cells, leading to a significant enhancement in MMCT efficiency. We initially treated two independent cell lines with various concentrations of TR and determined the optimal concentration for enhanced MMCT efficiency. Next, given the highly efficient outcomes reported with various virus envelope-based MMCT methods,<sup>15</sup> we examined the compatibility of TR with these procedures. To gain mechanistic insights, the duration of microtubule formation dynamics and mitotic arrest were analyzed, demonstrating contribution of TR to the improvement of the micronucleation rate. Furthermore, because human induced pluripotent stem cells (iPSCs)<sup>24</sup> are valuable tools for regenerative medicine, drug discovery, and developmental biology research, we examined the transfer of the human artificial chromosome (HAC)<sup>2</sup> from CHO cells to human iPSCs using an amphotropic virus (AmV) envelop protein from murine leukemia virus, and we determined that the efficiency of membrane fusion was increased.<sup>16,25</sup> Collectively, our novel procedure described herein showed enhanced MMCT efficiency through an improved micronucleation rate, as well as compatibility with virus envelope-based MMCT, including the generation of human iPSCs containing HAC. This procedure provides an alternative approach that advances chromosomal engineering technology and the use of HAC in genetic and regenerative medical research.

## RESULTS

### Evaluation of TR combined treatment

We tested two donor cell lines carrying different HACs (CHO-21HAC2<sup>2</sup> or CHO-BHIG11<sup>26</sup>) to assess micronucleation (Figure 1A). Schematic illustrations of the HACs are shown in Figures S1A and S1B. These cell lines have been used as models to evaluate chromosome transfer efficiency.<sup>6,11–14</sup>

First, CHO-21HAC2 cells were treated with Taxol (3, 25, 100, and 400 nM) and reversine (500, 1,000, 1,500, and 2,000 nM) for 3 days, and the induction of numerous small micronuclei in the CHO cells was observed with the combination of 100 and 400 nM Taxol and each concentration of reversine when compared with conventional colcemid treatment (Figures 1B, S2, and S3). Slight micronucleation was observed with combinations of 3 nM and 25 nM Taxol and 500, 1,000, 1,500, and 2,000 nM reversine, suggesting that TR promoted micronucleation in a dose-dependent manner (Figures S2A and S2B). Multiple small nuclei were identified within a single cell when analyzed under a confocal microscope (Figures 1C, S3A, and S3B). Quantitative evaluation was performed by Giemsa-staining analysis of micronuclei spreads to determine the optimal treatment concentrations of TR. The combination of 400 nM Taxol and 500 nM reversine (T400 + R500) had the highest micronucleation efficiency with a rate of  $76.7\% \pm 6.1\%$  of CHO-21HAC2 cells exhibiting the formation of five or more micronuclei (Figures 1D and S4 and Table S1). This micronucleation efficiency was significantly higher than that of conventional colcemid treatment ( $28\% \pm 2\%$ ) ( $p < 0.01$ ).

To assess the generality of micronuclei induction by TR treatment, another CHO clone was evaluated. TR treatment also demonstrated

high efficiency in CHO-BHIG11 cells (Figure S5). However, CHO-BHIG11 cells had lower sensitivity to reversine than CHO-21HAC2 cells, and significant micronucleation was observed with combinations of 400 nM Taxol and 1,000–2,000 nM reversine (Figures S5A and S5B). Accordingly, quantitative evaluation by Giemsa-staining analysis of micronuclei spreads revealed that treatment with T400 + R1500 promoted the optimal micronucleation induction rate ( $44\% \pm 5.3\%$ ) (Figures S5C, S6, and S7 and Table S2). This efficiency was also clearly higher than that of conventional colcemid treatment ( $9.3\% \pm 6.1\%$ ) ( $p < 0.05$ ) (Figure S5D).

In addition, the combination of colcemid and reversine decreased micronucleation in CHO-21HAC2 cells (Figure S8), indicating that reversine was effective with Taxol but not with colcemid. In CHO-21HAC2 cells, the micronucleation efficiency following the combined treatment with TN-16 and griseofulvin (TN + Gri)<sup>14</sup> was lower than that observed after treatment with TR (Figure S9A). Overall, the optimal concentration of TR treatment efficiently induced micronucleation in two independent CHO cell lines: CHO-21HAC2 cells at 400 nM Taxol and 500 nM reversine and CHO-BHIG11 cells at 400 nM Taxol and 1,500 nM reversine.

### Analysis of MMCT efficiency

We next attempted to determine whether micronucleation efficiency affected MMCT efficiency. We used CHO donor cells containing HACs (CHO-21HAC2 and CHO-BHIG11) and a benchmark recipient human fibrosarcoma (HT1080) cell line as well as CHO donor cells containing a mouse artificial chromosome (MAC; CHO-MAC1<sup>27</sup>) and a benchmark recipient mouse fibroblast (NIH3T3) cell line. The HACs and MAC harbor antibiotic resistance genes (Figures S1A–C), and when the intact artificial chromosomes or fragments containing resistant genes are introduced into recipient cells via microcells and micronuclei, drug-resistant colonies are produced. The number of drug-resistant colonies per experiment was determined and compared using each micronucleation condition (Figure 2A). MMCT efficiency was defined as the colony formation rate of recipient cells after fusion with microcells obtained from one to six T-25 culture flasks for each CHO cell line expressing each virus envelope (Table S3), i.e.,  $10^{-6}$  to  $10^{-4}$ , 1 to 100 colonies/ $10^6$  recipient cells using a standard protocol with colcemid as previously reported.<sup>11–15</sup> Microcells derived from CHO-21HAC2 were isolated using cytochalasin B and fused with HT1080 cells using measles viral (MV) fusogen, which induces cell membrane fusion mediated by an MV receptor, CD46.<sup>11</sup> Treatments with T400 + R500 and T400 + R1500 promoted significant improvements in MMCT efficiency with 7.7- and 4.5-fold increases ( $p < 0.01$ ), respectively, compared with colcemid treatment (Figures 2B and S10A and Table S3). These results indicated a positive relationship between micronucleation and MMCT efficiencies (Figure S11) ( $R^2 = 0.852$ ). Furthermore, MMCT efficiency was significantly improved in all donor cell lines with different fusogens, including MV (CHO-BHIG11/MV and CHO-21HAC2/MV cells) and ecotropic virus (EcoV) envelope (CHO-MAC1/EcoV cells) proteins, which induce cell membrane fusion mediated by an EcoV receptor, the murine cationic amino acid transporter-1 (mCAT-1), in NIH3T3 cells.<sup>13</sup>

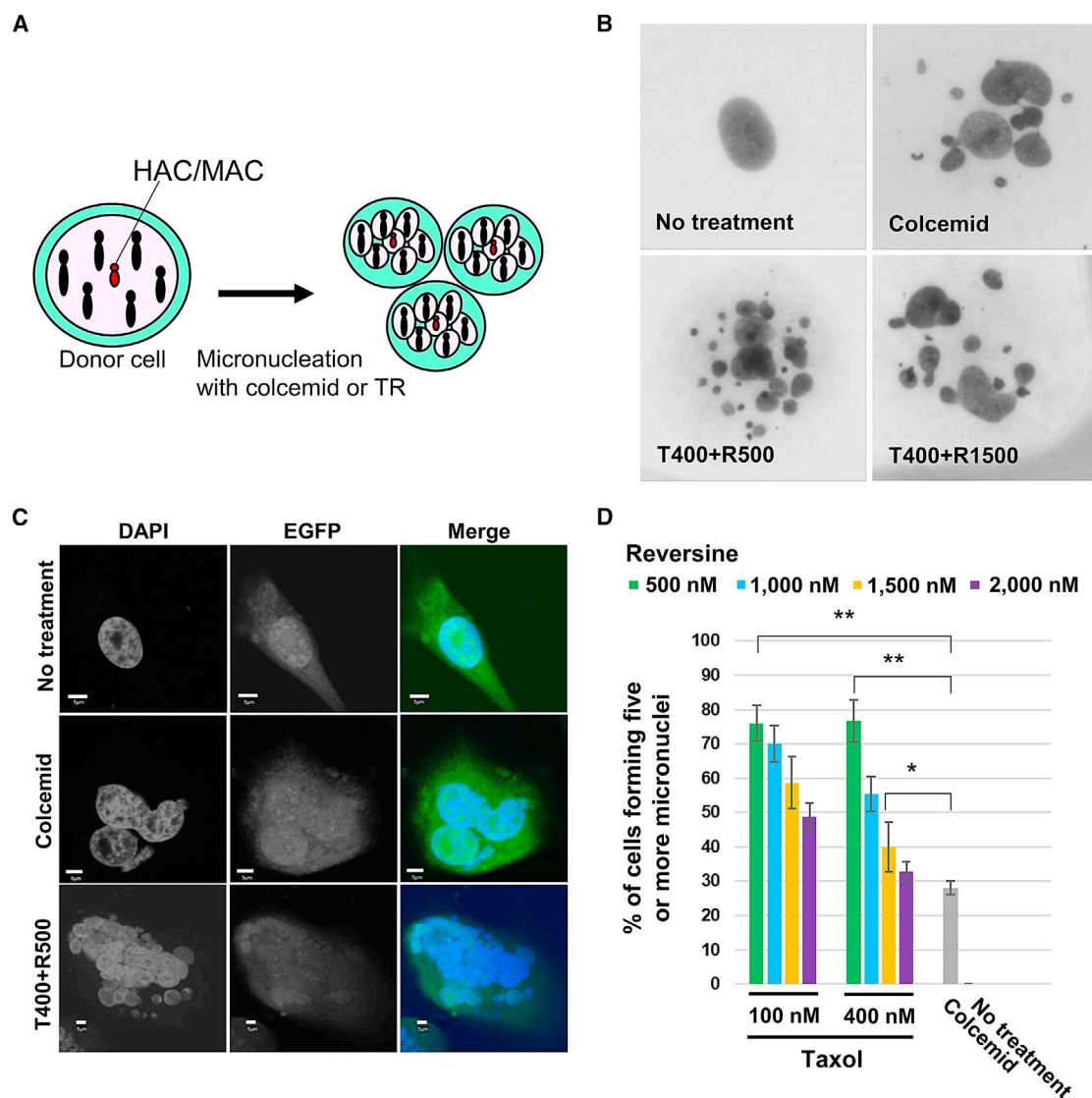


**Figure 1. Efficient induction of micronucleation by Taxol and reversine combined treatment**

(A) Schematic illustration of micronucleation after co-treatment with Taxol and reversine (TR) (HAC or MAC, human or mouse artificial chromosomes). (B) Representative images of Giemsa-stained micronuclei spreads of CHO-21HAC2 cells treated with reagents and used for quantitative evaluation of the micronucleation rate per cell. The results presented are representative images of experiments performed under the following conditions: untreated, colcemid, Taxol 400 nM + reversine 500 nM (T400 + R500), and Taxol 400 nM + reversine 1,500 nM (T400 + R1500). Figure S2 provides an overview of the experimental results. Because Carl Zeiss microscopes and the Ikaros software image acquisition system do not allow the insertion of a scale bar in these images, the image size was estimated using the “No treatment” images or the chromosome spread presented in Figure S2B, labeled “Chromosomes.” When the concentration of Taxol was set at 400 nM, slight needle-like crystals occasionally occurred, indicating that this concentration was the maximum useful concentration. (C) Morphological analysis of CHO cells after chemical compound treatment. The images of no treatment, colcemid (0.1  $\mu\text{g}/\text{mL}$ ), and co-treatment with T400 + R500 are indicated. Green represents EGFP fluorescence indicating the cytoplasm. Blue represents DAPI fluorescence staining, which labels the nucleus. Figure S3 provides an overview of the experimental results. The scale bar indicates 5  $\mu\text{m}$ . (D) The micronucleation efficiency of CHO-21HAC2 cells was analyzed after treatment with different combinations of Taxol (100 and 400 nM) and reversine (500, 1,000, 1,500, and 2,000 nM). Additionally, the micronucleation efficiency was evaluated after treatment with colcemid (0.1  $\mu\text{g}/\text{mL}$ ). Fifty cells were analyzed for each experiment, and the percentage of cells that formed five or more micronuclei was quantified. Each experiment was conducted three times. The error bars indicate the standard deviation (SD). Statistical significance was determined using the Student's t test (\* $p < 0.05$ , \*\* $p < 0.01$ ).

MMCT efficiency using CHO-BHIG11/MV was increased 18.3-fold ( $p = 0.152$ ), and CHO-MAC1/EcoV was increased 4.9-fold ( $p < 0.05$ ), respectively (Figures 2C, 2D, and S10B and Table S3). The

TN + Gri treatment increased MMCT efficiency 3.7-fold ( $p < 0.05$ ), in accordance with a previous report,<sup>14</sup> although there was no noticeable improvement in micronucleation efficiency (Figure S9B).

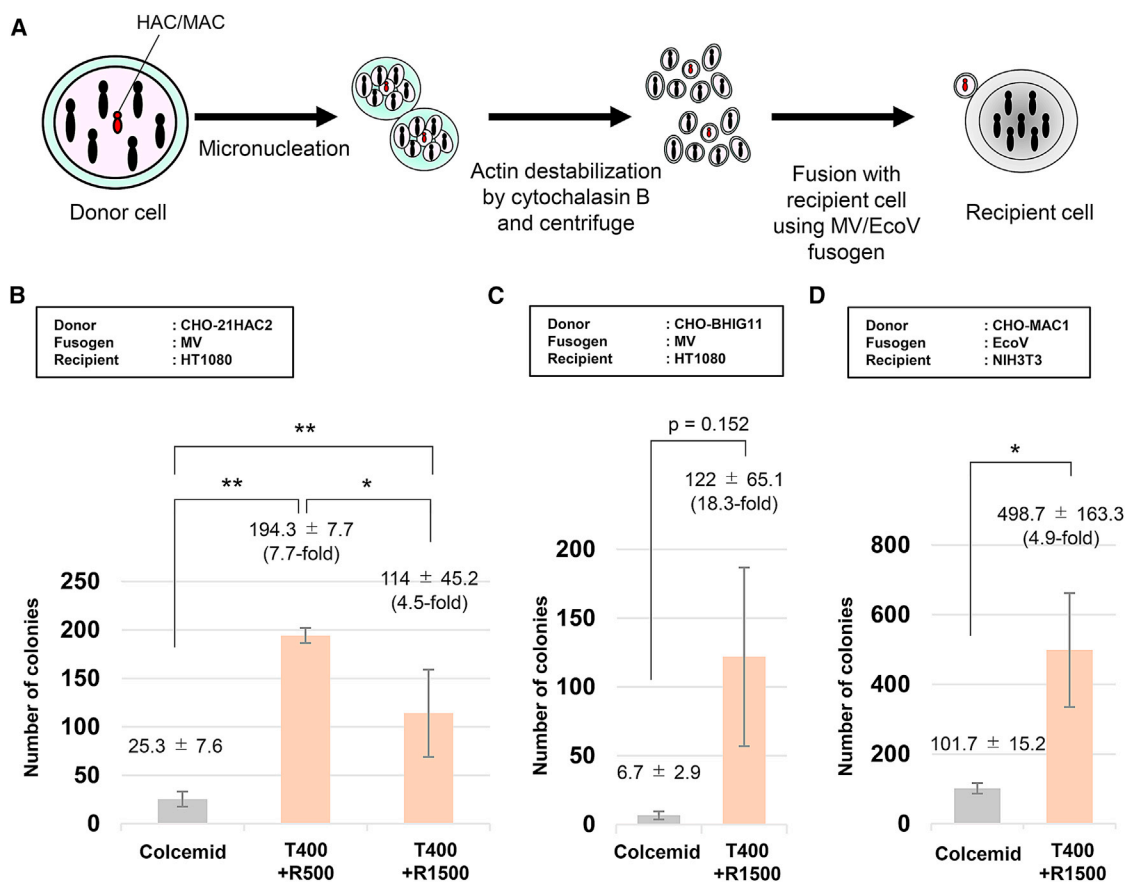


**Figure 2. Assessment of MMCT efficiency**

(A) Schematic illustration of the assessment of MMCT efficiency. (B) Comparison of the MMCT efficiency between treatments with colcemid (0.1  $\mu\text{g}/\text{mL}$ ) ( $n = 6$ ) and the combination of Taxol and reversine (T400 + R500 and T400 + R1500) ( $n = 3$ , each). The donor cells (CHO-21HAC2 cells), MV fusogen, and recipient cells (HT1080) are indicated in (C) and CHO-MAC1 donor and NIH3T3 recipient cells (D). Donor cells, pathogen, and recipient cells are shown in the square box above the figure (B–D). Statistical analyses were performed with the Student's *t* test (\* $p < 0.05$ , \*\* $p < 0.01$ ). The data are presented as the means  $\pm$  standard deviation.

### Retention rate of transferred HAC/MAC in recipient cells

We transferred 21HAC2 from CHO-21HAC2 donor cells to HT1080 recipient cells and MAC1 from CHO-MAC1 donor cells to NIH3T3 recipient cells using MMCT with each chemical compound treatment, i.e., the TR (T400 + R1500) or colcemid method. Subsequently, we performed PCR and fluorescence *in situ* hybridization (FISH) analyses to determine if one copy of the transferred normal HAC/MAC, which contained antibiotic-resistant genes, was retained independent of the host chromosomes. Through PCR analysis detecting selectable markers on 21HAC2 and MAC1 (Figures S1A and S1C), PCR analysis confirmed the presence of the selection markers on the HAC/MAC for all HT1080-21HAC2 cells (10 clones from the TR method #01–11, and 10 clones from the colcemid method #01–10) (Figures S12A and S12B) and NIH3T3-MAC1 cells (9 clones from the TR method #01–11 and 10 clones from the colcemid method #01–10) (Figures S12C and S12D). Therefore, it can be inferred that almost all drug-resistant colonies that appeared as a result of drug selection were due to the introduction of HAC/MAC. Next, FISH analysis was performed

on these clones to verify the independent transfer of HAC/MAC (Figures 3A–3H), as the introduced chromosome can occasionally translocate to the host chromosomes.<sup>28</sup> For each clone, 40 metaphase cells were analyzed. In cases where 21HAC2/MAC1 was introduced into recipient HT1080 or NIH3T3 cells using colcemid or TR, the morphology of 21HAC2/MAC1 observed within the donor cells (as shown in Figure 3A for 21HAC2 and Figure 3F for MAC1) and the staining properties of the DNA probes (p11-4<sup>29</sup> or pVGNLH1<sup>30</sup>) were comparable with the morphology and staining properties in the recipient cells. No alterations were observed in the karyotype of the host cells pre- and post-introduction of 21HAC2/MAC1 (as shown in Figure 3B for HT1080 and Figure 3F for NIH3T3). The observed examples of chromosome abnormalities are listed in Figure S12. The percentage of cells that retained normal HAC/MAC was calculated after excluding cells in which HAC/MAC had translocations (Figure S13A) or amplifications (Figures S13B and S13C). The results of FISH analysis for HT1080-21HAC2 (Table S4) and NIH3T3-MAC1 (Table S5) clones, which underwent MMCT using the colcemid or TR method, are

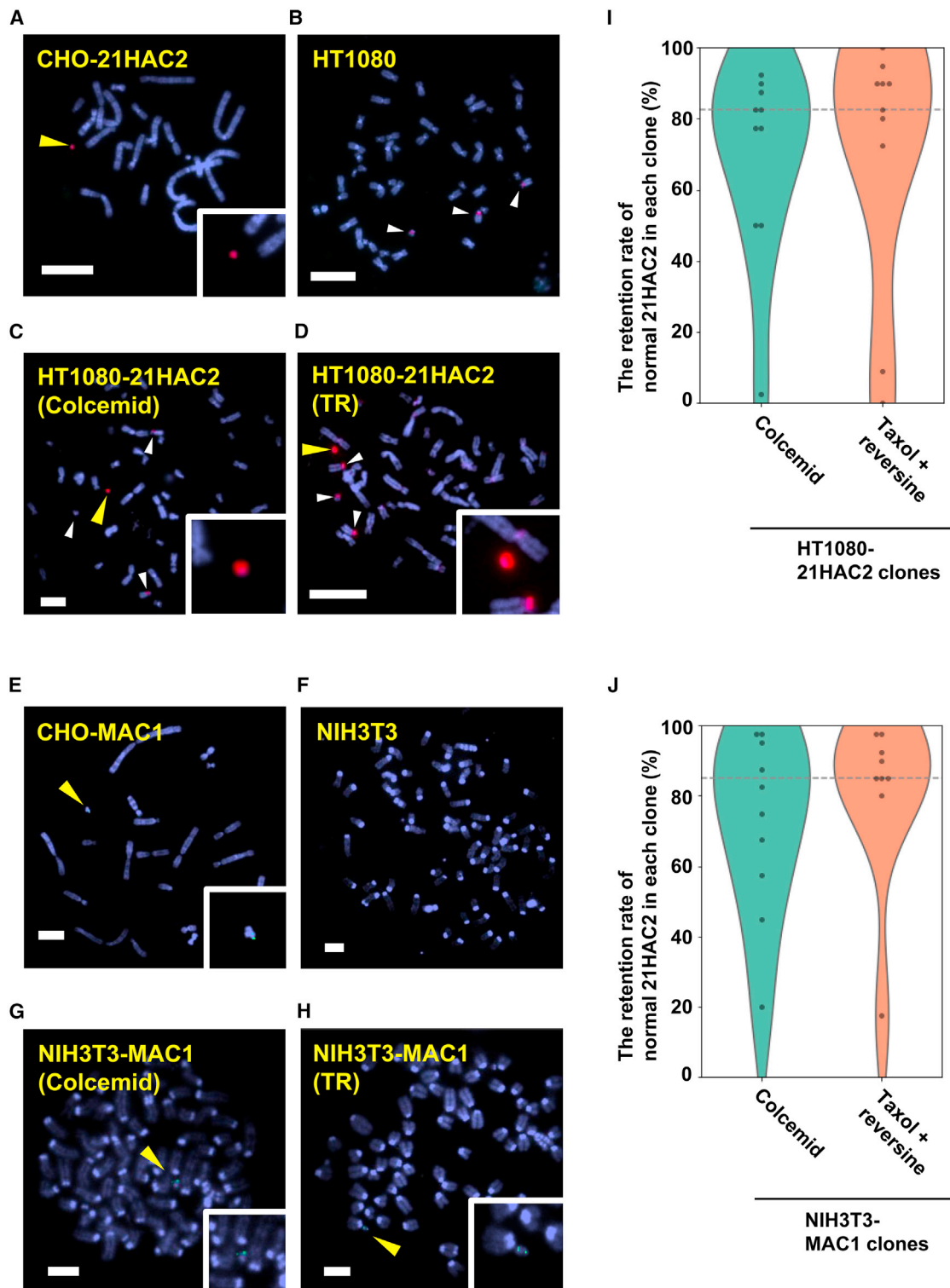


**Figure 3. Fluorescence *in situ* hybridization (FISH) analysis**

FISH analysis of (A) CHO-21HAC2/MV donor cells and (B) HT1080 recipient cells. FISH analysis of HT1080 cells carrying 21HAC2, which was transferred from CHO-21HAC2/MV cells with colcemid (C) and the TR (D) method. The yellow arrowheads indicate 21HAC2, and white arrowheads indicate chromosomes 13 and 21. An enlarged image of 21HAC2 is shown. The red fluorescence represents the digoxigenin-labeled p11-4 probe that indicates the alpha satellites of chromosomes 13 and 21.

(legend continued on next page)

summarized elsewhere. The median retention rate of 21HAC2 transferred from CHO-21HAC2/MV in single cloned HT1080 cells was  $90\% \pm 27.9\%$  ( $n = 10$  clones) and  $90\% \pm 29\%$  ( $n = 10$  clones) using the colcemid or TR method, respectively (Figure 3I). The median retention rate of MAC1 transferred from CHO-MAC1/EcoV in single cloned NIH3T3 cells was  $78.8\% \pm 25.5\%$  ( $n = 10$  clones) and  $85\% \pm 24.6\%$  ( $n = 9$  clones) using the colcemid or TR method, respectively (Figure 3J). There was no significant difference between the median retention rates using the Mann-Whitney *U*-test; however, the retention rate after TR treatment tended to be higher than that after colcemid treatment. Thus, compared with the conventional colcemid method, the TR method achieved chromosome transfer without inducing notable chromosomal abnormalities in HT1080-21HAC2 cells and NIH3T3-MAC1 cells.

### Chromosomal transfer from CHO cells to human iPSCs

Human iPSCs are attractive for studies on regenerative medicine; however, the transfer of HAC from CHO cells to iPSCs remains inefficient.<sup>6,16,31,32</sup> To assess MMCT efficiency for human iPSCs, micronucleation was induced by the TR method (T400 + R1500) in CHO-modified 21HAC2 cells<sup>5</sup> that expressed AmV13 fusogen (CHO-modified 21HAC2/AmV cells). The resulting microcells were fused to human iPSCs via sodium-dependent phosphate transporter-2 (PIT-2),<sup>13</sup> which is the receptor for the AmV-fusogen (Figure 4A). AmV is a different protein from MV and EcoV, and it can be used for MMCT into mammalian cells other than human cells. Therefore, we also investigated whether the TR method is useful for MMCT to human iPSCs (201B7)<sup>24</sup> as recipient cells. The TR method produced an average of 4.7 HAC-transferred clones per fusion, but the colcemid method failed to produce any clones (Table 1). The expression of enhanced green fluorescence protein (EGFP), the gene for which was present on the HAC, was clearly observed in the obtained iPSCs (Figure 4B). PCR analysis to detect selectable markers on the modified 21HAC2 (Figure S1D) confirmed that the selection marker gene was present on the modified 21HAC2 for all five clones obtained by the TR method (Figure S12E). FISH analysis showed that the HAC was independently retained among the normal host chromosomes (Figure 4C). Thus, the MMCT of HAC from donor cells to iPSCs, which rarely occurs with colcemid treatment,<sup>16</sup> may now be achieved efficiently using the TR method. This finding will substantially support the application of processed chromosomes, such as HAC, in regenerative medicine research.

### Mechanisms of effective micronucleation

We treated CHO cells with reversine and colcemid or Taxol (Figures 1D and S8) to investigate which factors contributed to the observed results, given that the TR treatment promoted highly efficient micronucleation. Colcemid treatment usually promotes micronucleation by causing prolonged mitotic arrest, which results in cells that slip out of mitosis and form micronuclei.<sup>20</sup> Taxol is a major microtubule stabilizer, and reversine treatment induces mitotic slippage. Therefore, we focused on cell-cycle analysis to understand the mechanism of increased micronucleation after TR treatment. We previously reported that during the process of advanced micronucleation, cells treated with colcemid underwent multiple rounds of M phase.<sup>20</sup> Analogous to the well-studied effect of M-phase arrest by nocodazole and M-phase slippage-inducing effects of reversine in HeLa cells,<sup>21</sup> we confirmed the M-phase slippage-inducing effect of reversine when used in combination with colcemid or Taxol in CHO cells during long-term treatment involved in MMCT. We also observed dynamic changes in microtubule formation in CHO cells. Time-lapse imaging was used to examine micronuclei formation in CHO cells expressing the histone H2B-GFP,<sup>20</sup> which fluorescently labels nuclei, as shown in Videos S1, S2, S3, S4, S5, and S6. The time-lapse images obtained were analyzed to calculate the duration of mitotic arrest per cell (Figure 5A). In CHO cells expressing H2B-GFP, the duration of mitotic arrest was evaluated based on cell rounding and nuclear disappearance. In untreated CHO cells, the median duration of the metaphase was  $27.0 \pm 14.2$  min. However, after a single treatment with colcemid and Taxol, the median metaphase durations were significantly elongated, with values of  $240.0 \pm 162.2$  min and  $163.5 \pm 43.5$  min, respectively ( $F(5,99) = 45.4383$ ,  $p < 0.0005$ ) (Videos S1, S2, and S3). The duration of the metaphase was 3.0–15.0 min in CHO cells treated with reversine (Video S4). In CHO cells treated with reversine and colcemid, the duration of the metaphase was  $15.0 \pm 8.8$  min, and with regard to the formation of micronuclei, a single large nucleus was observed, and multiple micronuclei were not observed (Video S5). However, in CHO cells treated with TR, the duration of the metaphase was  $18.0 \pm 11.5$  min, and multiple micronuclei were observed (Video S6). These results suggest that the combined treatment with reversine significantly suppressed the prolongation of mitosis caused by colcemid and Taxol ( $p < 0.0005$ ). However, the micronucleation ability was higher with the combined TR treatment, as also evidenced by time-lapse images. CHO cells treated with TN + Gri exhibited shortened mitotic arrest and slight micronucleation (Video S7).

---

21HAC2 was derived from chromosome 21 and stained with the p11-4 probe.<sup>29</sup> The light-blue color indicates DAPI-stained chromosomes. When the HT1080 cell line was analyzed using the p11-4 probe, it was common to observe a total of three signals indicating chromosomes 13 and 21. It is thought that one of the two copies of chromosome 21 has low staining because of a chromosomal polymorphism. FISH analysis of (E) the CHO-MAC1/EcoV cell line as a donor cell and (F) NIH3T3 cell line as a recipient cell. FISH analysis of NIH3T3 cells containing the mouse artificial chromosome MAC1, which was transferred from CHO-MAC1/EcoV cells after treatment with colcemid (G) and the TR method (H). The yellow arrowheads indicate MAC1, and the insets show enlarged images of MAC1. The green fluorescence represents biotin-labeled pGNLH1 containing a Neo-resistant gene.<sup>27</sup> The light-blue color indicates DAPI-stained chromosomes. (I) The retention rates of normal HACs/MACs were evaluated by FISH analysis in HT1080 cells with 21HACs obtained with colcemid ( $n = 10$  clones) or the TR method ( $n = 10$  clones) and (J) NIH3T3 cells with MAC1 retention ( $n = 10$  clones for the TR method and  $n = 9$  clones for the colcemid method). All clones were analyzed for 40 metaphase cells each. The graph shows the percentage of cells with normal HACs/MACs detected in each clone. Each dot represents the retention rate of individual clones. The dashed line represents the median value across all clones. A Mann-Whitney *U*-test was performed, but no significant difference was observed.

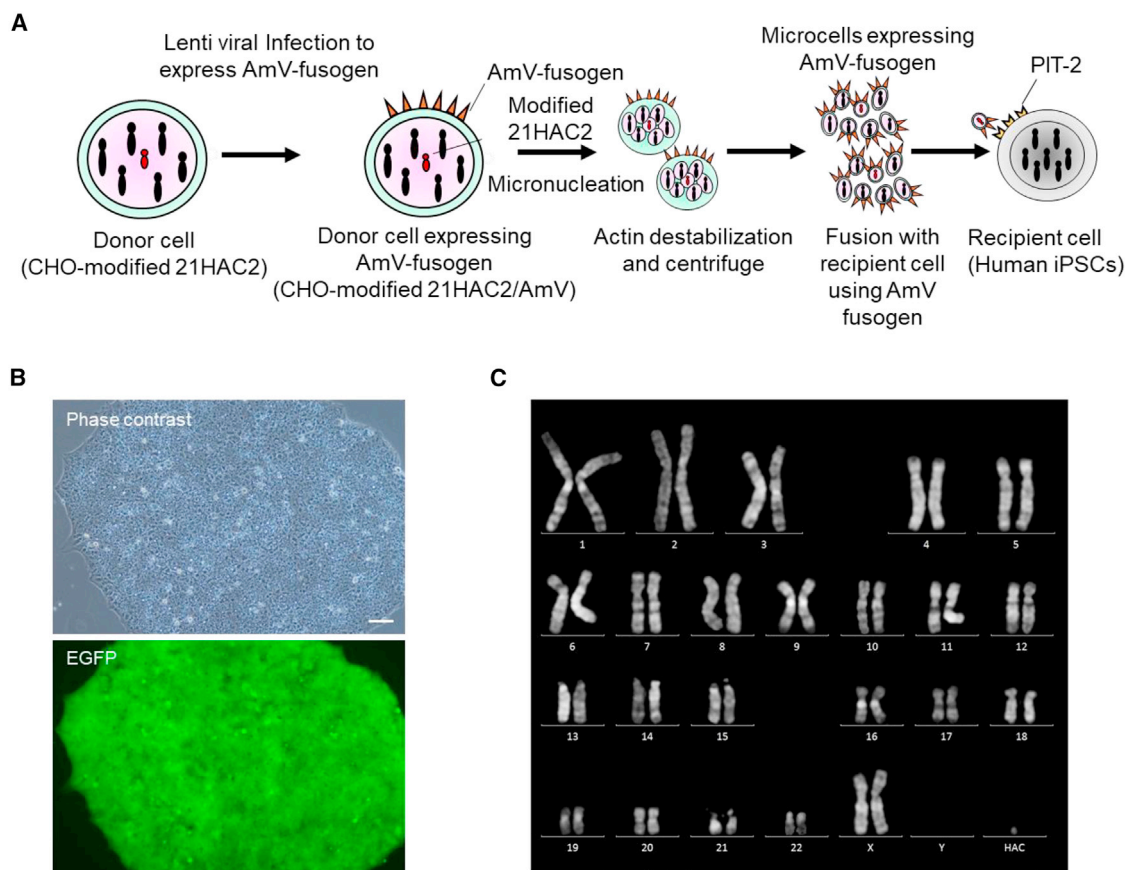


**Figure 4. MMCT from CHO-modified 21HAC2 donor cells to human iPSCs as recipient cells**

(A) Schematic illustration of MMCT of modified-21HAC2 from CHO-modified 21HAC2 donor cells to recipient human iPSCs (201B7).<sup>24</sup> The AmV-fusogen was transduced using a lentivirus vector<sup>13</sup> to generate CHO-modified 21HAC2/AmV donor cells. PIT-2, a receptor for AmV-fusogen, was constitutively expressed on the recipient human iPSCs. (B) Representative phase contrast and fluorescent images of a human iPSC clone obtained by the TR method. Upper: phase contrast microscopy. Lower: EGFP fluorescence microscopy. The scale bar indicates 100  $\mu\text{m}$ . (C) Karyotypic analysis of the human iPSC clone by Q-banding.

EGFP-labeled alpha-tubulin was used to image microtubule formation during mitosis after treatment with each chemical compound (Figure 5B). Under normal cell culture conditions, metaphase cells contained chromosomes that were aligned along the equatorial plane and spindle threads that were attached to chromosomes from both poles (Figure 5B, untreated). In colcemid-treated cells, spindle elongation and attachment to chromosomes were not observed in most mitotic cells because of the inhibition of spindle formation (Figure 5B, colcemid). Taxol treatment induced excessive spindle fibers and multiple acentrosomal spindle pole formation, and chromosome alignment in the middle of the polar spindle was disturbed (Figure 5B, Taxol). Spindle threads were formed from both poles by reversine treatment but were not attached to most chromosomes, and chromosomes were not aligned along the equatorial plane (Figure 5B, reversine). TR treatment induced excessive spindle formation with more than two spindle poles. Bipolar spindles were formed, but the chromosomes were not aligned along the equatorial plane. These results indicated that spindle multipolarization during mitosis by Taxol promoted micronuclei formation while inhibiting cell-cycle progression.

Reversine canceled the inhibition of cell-cycle progression by Taxol regardless of microtubule formation status during mitosis leading to efficient micronucleation. Colcemid treatment induced micronucleation via elongated metaphase arrest by activating the SAC-related proteins (Figure 6A); however, this effect was prevented as reversine

**Table 1. The number of iPSC colonies obtained by MMCT after colcemid or Taxol and reversine combined treatment (T400 + R1500)**

	Number of colonies	
	T400 + R1500 treatment (MMCT efficiency)	Colcemid
Experiment 1	7 ( $1.4 \times 10^{-5}$ )	0
Experiment 2	5 ( $2.0 \times 10^{-5}$ )	0
Experiment 3	2 ( $5 \times 10^{-5}$ )	0
Average	4.7 ( $2.1 \times 10^{-5}$ )	0

The experiments were performed in triplicate.

Abbreviations: iPSC, induced pluripotent stem cells; MMCT, microcell-mediated chromosome transfer; R1500, 1,500 nM reversine; T400, 400 nM Taxol.

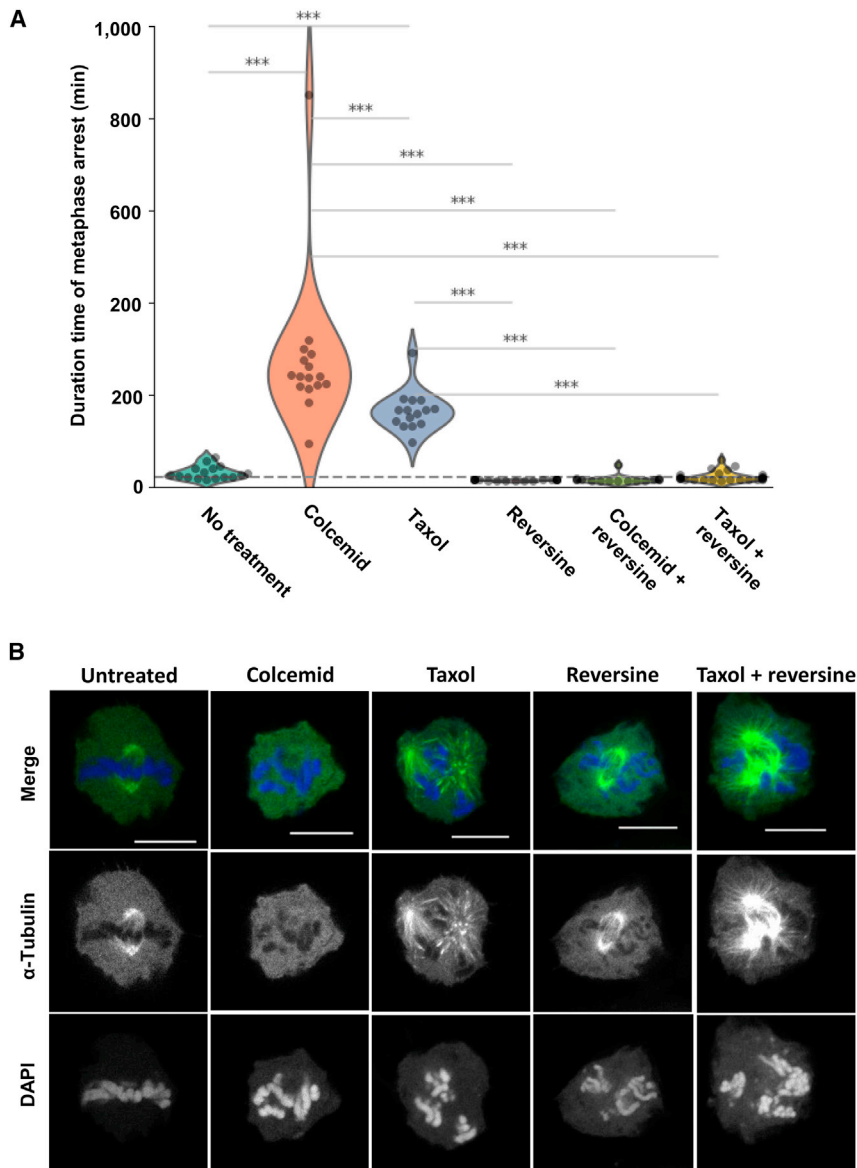


**Figure 5. Analysis of metaphase arrest by chemical compounds**

(A) Measurements of the mitotic arrest period using time-lapse analysis. The time (min) during which the spherical state was maintained while the cells changed from an adherent to spherical form and back again during mitosis was detected using time-lapse imaging. The duration of the spherical state is indicated using beeswarm and violin plots. The dotted lines in the graph represent the mean values. The x axis indicates the treatment conditions, and y axis indicates the observed mitotic arrest time (min). The following six conditions were used: compound-free culture ( $n = 16$  cells),  $0.1 \mu\text{g/mL}$  colcemid ( $n = 16$  cells),  $400 \text{ nM}$  Taxol ( $n = 15$  cells),  $1,500 \text{ nM}$  reversine ( $n = 17$  cells),  $0.1 \mu\text{g/mL}$  colcemid and  $1,500 \text{ nM}$  reversine combination ( $n = 16$  cells), and  $400 \text{ nM}$  Taxol and  $1,500 \text{ nM}$  reversine combination ( $n = 27$  cells). The Tukey-Kramer post-hoc test was performed for statistical analysis, and the data were evaluated using analysis of variance;  $F(5,99) = 45.4383$ .  $***p < 0.001$ . (B) Representative images of microtubules using EGFP-alpha-tubulin under each treatment condition. The cells were untreated or treated with  $0.1 \mu\text{g/mL}$  colcemid,  $400 \text{ nM}$  Taxol,  $1,500 \text{ nM}$  reversine, and a combination of  $400 \text{ nM}$  Taxol plus  $1,500 \text{ nM}$  reversine. The merged images are displayed in the upper section. The green color indicates EGFP (the middle section) and blue indicates DAPI-staining (the lower section). Scale bar represents  $10 \mu\text{m}$ .

conventional colcemid method, although we observed varying drug sensitivities among multiple CHO cell lines wherein CHO-BHIG11 cells showed a lower response to reversine than CHO-21HAC2 cells, resulting in high micronucleation rates at high concentrations. Significant clonal variation of CHO cells is caused by genomic instability<sup>33</sup>; therefore, assessing the micronucleation rate within the  $500\text{--}2,000 \text{ nM}$  range for reversine is important when working with a new CHO clone (Figures 1D, 2B, 2C, and S7).

We propose the mechanism by which efficient micronucleus induction occurs as follows.

Regarding the process of micronucleation by conventional colcemid treatment, micronuclei are formed by pseudo-cell-cycle progression that does not involve cytoplasmic division. Because there is no cytoplasmic division, the cell cycle progresses, and the number of chromosomes per cell doubles each time it passes through the pseudo-S phase, resulting in the formation of additional micronuclei.<sup>20</sup> Observations from the time-lapse imaging suggested that a similar pseudo-cell-cycle progression occurred with the TR treatment. Notably, the combination of TR may induce chromosome segregation by (1) generating Taxol-induced mitotic microtubule asters, which results in multipolar spindle, ectopic chromatin surface exposure, and marked micronucleation via the nuclear membrane formation of individual chromosomal regions,<sup>21</sup> and (2) inhibiting the mitotic

inhibited the SAC. Furthermore, co-treatment with TR treatment resulted in the formation of micronuclei via induced micronucleation by synergistically affecting chromosomal polarization and mitotic slippage (Figure 6B), indicating that efficient micronucleation was achieved by a completely different mechanism.

## DISCUSSION

In this study, we demonstrated an improvement in micronucleus formation efficiency by TR treatment and the subsequent enhancement of MMCT efficiency in CHO cells. Upon optimizing the TR concentration, treatment with  $400 \text{ nM}$  Taxol and  $500 \text{ nM}$  reversine for CHO-21HAC2 and  $400 \text{ nM}$  Taxol and  $1,500 \text{ nM}$  reversine for CHO-BHIG11 resulted in more efficient micronucleation than the



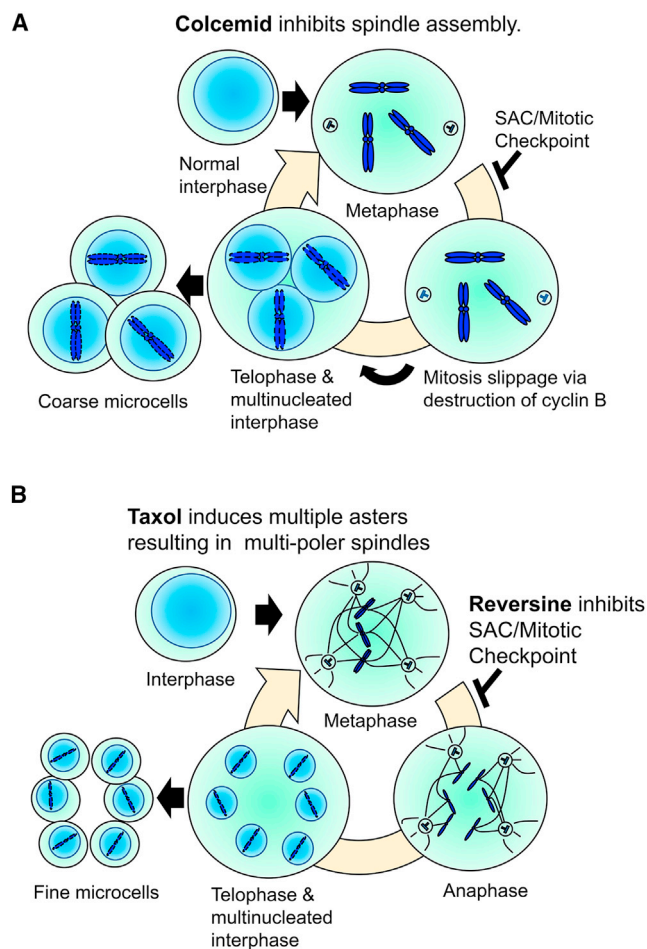


**Figure 6. A model of the micronucleation process with different chemical compounds**

(A) Colcemid inhibits spindle assembly, which activates the SAC and results in prolonged mitotic arrest. In mitosis-arrested cells, chromosomes are time-dependently dispersed and multinucleated in the interphase. (B) A model of micronucleation after co-treatment with TR. Taxol induces multipolar mitotic spindles. The multipolar spindles elongate from multiple asters and promote chromosome dispersion in mitotic cells. SACs that are activated in spindle-forming aberrant cells are inhibited by reversine, leading to mitotic escape and pseudo-cell-cycle progression.

checkpoint by reversine, which presumably shortens the long mitotic phase of normal proliferative cells (usually 30–60 min), resulting in a relative decrease in the proliferation index, although this inhibition also promotes cell-cycle progression and increases the proportion of cells with micronuclei (Figure 5A). Thus, efficient micronucleation is presumed to occur in the presence of a combination of reagents that cause multipolarization in mitosis and shortening of the mitotic phase.

Although efficient micronucleation was achieved by TR treatment in this study, identifying compounds with mechanisms of action similar to Taxol and/or reversine might induce micronuclei at lower concen-

trations and lead to universally applicable drug treatments across various CHO clones. Substitutes for Taxol include Docetaxel,<sup>34</sup> and for reversine, AMG-900.<sup>35</sup> Substitutes for reversine, such as a combination of Arisertib specific for Aurora A<sup>36</sup> and Barasertib specific for Aurora B<sup>37</sup> might be an alternative method. By examining the optimal concentration and treatment time, it may be possible to discover agents that induce micronuclei formation more efficiently than the TR method. Studies using drugs other than TR will be important when examining cells such as iPSCs, where the induction of micronucleation has not been well established.

To establish cells containing a certain target chromosome transferred via MMCT, it is necessary to selectively isolate microcells that retain only target chromosomes such as HAC/MAC. An important feature of this method is the formation of small micronuclei containing a single chromosome. Furthermore, the size of micronuclei was reported to correlate with the total amount of DNA contained within them, reflecting the size and number of chromosomes.<sup>38</sup> Indeed, the number of small micronuclei appeared to increase under T400 + R500 treatment conditions (Figures 1B and 1C). In this study, microcells were sorted by size using filters with pore sizes of 8, 5, and 3  $\mu\text{m}$  during the purification process of the MMCT method, which might have increased the ratio of microcells retaining and packaging only HAC/MAC. This is because the size of micronuclei containing HAC/MAC is expected to be small, and thus, the filtration step removes microcells containing relatively large CHO chromosomes. This might result in an enrichment of microcells containing HAC/MAC leading to improved MMCT efficiency. In cases where the introduction of a large chromosome is desired, this method can be used to induce the formation of micronuclei containing a single chromosome, followed by the isolation of microcells of an appropriate size. Therefore, the induction of small micronuclei and subsequent improvement of microcell production, which is expected to contain a single chromosome, is important for the development of drug treatment methods that improve MMCT efficiency.

In addition, chromosomal damage that occurs during micronucleation should be noted.<sup>28</sup> As expected, the clones analyzed in this study retained drug-resistance genes (Figure S12), and FISH analysis demonstrated normal HAC/MACs were introduced at a frequency comparable with the colcemid method (Figures 3I and 3J). Therefore, our results suggested that the TR method does not induce additional chromosomal damage. However, we observed that TN + Gri treatment did not significantly affect the micronucleation efficiency (Figure S9A) but confirmed the improved MMCT efficiency by 3.7-fold (Figure S9B). These results indicate that efficient micronucleation and reduced DNA damage are important for MMCT efficiency, and that the TR method can be improved further. The assessment of chromosome damage is an essential consideration; however, a comprehensive study such as quantitative next-generation sequencing-based telomere-to-telomere assembly<sup>39</sup> is needed to evaluate the efficiency of transferring intact, complete chromosomes to detect chromosomal damage that is not identifiable by microscopy.<sup>7</sup>

To translate the results of this research into the development of regenerative medicine, the MMCT efficiency in iPSCs must be improved. In the current study, HAC/MAC were transferred from CHO cells to iPSCs but at a low frequency (2–7 clones/experiment) (Figures 2B and 2C and Table 1). It was reported that increasing the ratio of microcells to recipient cells (reducing the iPSC density) improved the efficiency of MMCT,<sup>16</sup> but the principle has not been clarified yet. In addition to the increased formation of small micronuclei and enrichment of microcells by the TR method for improved MMCT efficiency, it is noteworthy that although the efficiency of virus envelope-based MMCT might be dependent on the receptor expression levels on the plasma membrane of the recipient cells, the iPSCs examined in this study expressed PIT-2 at a high frequency and level (data not shown) but demonstrated lower efficiency of chromosome transfer. These findings suggest additional cellular processes are associated with the acceptance of chromosomes in iPSCs. The rigorous evaluation and elucidation of molecular mechanisms will lead to improvements in MMCT efficiency among different recipient cells.<sup>15</sup>

In conclusion, although various improved MMCT methods have been reported,<sup>11–16</sup> our refined MMCT method using TR treatment significantly enhanced MMCT efficiency using CHO cells as donor cells. Regarding the augmentation of MMCT efficiency, the use of tissue culture plastics treated with collagen/laminin to fortify cell adhesion and the substitution of cytochalasin B with the actin destabilizer latrunculin B have shown promising results.<sup>14</sup> Integrating the TR method with these factors might enhance MMCT efficiency even further. Although previously reported chromosome donor cells have been limited to CHO, A9 cells, or human cancer cells, the TR method might induce micronucleation in cell types that were previously unsuitable as chromosome donor cells. Regarding recipient cell lines, it is now possible to improve the utility of the HT1080 and NIH3T3, as well as iPSCs. The efficient production of cells with a normal karyotype and the HAC should greatly enhance regenerative medicine research using HAC. Thus, the TR method will allow a significant improvement in the efficiency of micronucleation in a variety of donor cells and the introduction of HAC/MAC into a variety of recipient cells. As such, the breakthroughs achieved in this study hold great promise in paving the way for the development of innovative MMCT methodologies.

## MATERIALS AND METHODS

### Ethics statement

This study was approved by the Recombinant DNA Experiment Safety Committee of Tottori University and Tokyo Metropolitan Institute of Medical Science prior to performing recombinant DNA experiments. All methods were performed in accordance with relevant guidelines and regulations.

### Cell culture

CHO cells were derived from a hypoxanthine phosphoribosyl transferase-deficient cell line (JCRB0218) (NIBIOHN; Osaka, Japan) and cultured in CHO culture medium consisting of Ham's F-12 medium (Fujifilm Wako; Osaka, Japan) supplemented with 10% fetal bovine

serum (FBS) (Biowest; Vieux Bourg, France) and 1% penicillin/streptomycin (Fujifilm Wako). CHO-K1 cells were the parental cell line of the CHO cells (JCRB9018) (NIBIOHN). CHO cells containing 21HAC2<sup>2</sup> and expressing measles virus (MV) hemagglutinin (MV-H) and fusion protein (F) (CHO-21HAC2/MV cells)<sup>11</sup> were cultured in CHO medium supplemented with blasticidin S (8 µg/mL; Fujifilm Wako) and G418 (800 µg/mL; Fujifilm Wako). CHO cells containing MAC or HAC, including CHO-MAC1/EcoV and CHO-modified 21HAC2/AmV cells,<sup>13</sup> were maintained in CHO medium supplemented with G418 (800 µg/mL). CHO cells containing tet-O HAC<sup>26</sup> were transfected with the pQCXIN-TetR-mCherry vector<sup>40</sup> (Addgene plasmid #59417; Addgene; Cambridge, MA, USA) and selected with 800 µg/mL G418 to obtain CHO cells expressing the mCherry-rtTA fusion protein. The established CHO-BHIG11 clone was transfected with vectors encoding MV-H, MV-F,<sup>11</sup> and the zeocin resistance gene and selected with 400 µg/mL zeocin. The established CHO-BHIG11/MV cells were maintained in CHO medium supplemented with G418 (800 µg/mL). Diagrams of HACs/MAC are shown in Figure S1. HT1080 cells (CCL-121) and NIH3T3 cells (CRL-1658) were purchased from the American Type Culture Collection (Manassas, VA, USA) and maintained in DMEM supplemented with 10% FBS and 1% penicillin/streptomycin. The iPSC line 201B7 (HPS0063)<sup>24</sup> was purchased from Riken BRC (Tsukuba, Japan) and maintained in StemFit AK02N (Takara Bio; Kusatsu, Japan) and iMatrix-511 Silk (Takara Bio) following the manufacturer's instructions.

### Treatment conditions for CHO cells

Colcemid solution (demecolcine) (10 µg/mL) was purchased from Fujifilm Wako. Taxol (Fujifilm Wako) was adjusted to 1 mM using 70% ethanol. Reversine (Cayman Chemical; Ann Arbor, USA) was adjusted to 1 mM using dimethyl sulfoxide (Fujifilm Wako). Micronucleation of CHO cell lines was induced by culturing in Ham's F-12 medium supplemented with 20% FBS in the presence of 0.1 µg/mL colcemid or 160 µM TN-16 (Santa Cruz Biotechnology; Dallas, TX, USA) combined with 50 µM griseofulvin (Santa Cruz Biotechnology) for 72 h or Taxol (Fujifilm Wako) and reversine at the indicated concentrations for 48 h. For the colcemid or TR combination, the medium was replaced with fresh medium and cultured for another 24 h.

### Observation of micronuclei by confocal microscopy

CHO cells were seeded at  $1 \times 10^4$  cells in a poly-lysine-coated slide chamber (Matsunami Glass Ind.; Kishiwada, Japan), and micronuclei formation was induced using the method described above. Then, 72 h after micronuclei induction, cells were fixed with 4% paraformaldehyde at room temperature for 15 min and washed with PBS. The cells were then stained with 4',6-diamidino-2-phenylindole (DAPI; 1.0 µg/mL; Merck Sigma-Aldrich; St. Louis, MO, USA) for 15 min and observed by a confocal microscope FV10i-DOC (Olympus; Shinjuku-ku, Japan) and analyzed by the attached software.

### Assessment of micronucleation efficiency

After inducing micronucleation, cells were fixed with Carnoy's solution (1:3 acetic acid:methanol) (both Fujifilm Wako) and spread on

glass slides (Matsunami Glass Ind.). The nuclei of cells were incubated with 5% Giemsa stain for 15 min (Fujifilm Wako) to assess the micronucleation rate. Images were captured using an Axio Imager Z2 fluorescence microscope (Carl Zeiss; Jena, Germany), and the number of micronuclei per cell was analyzed with the Ikaros software program (MetaSystems; Altlusheim, Germany). Each treatment was repeated three times, and 50 cells were evaluated in each repetition to determine the percentage of cells forming five or more micronuclei.

#### Measurement of the duration of metaphase arrest by live-cell imaging

CHO cells ( $5 \times 10^4$  cells) were seeded onto 35-mm glass-based dishes (AGC Techno Glass Co.; Kawashiri, Japan) and allowed to adhere for 24 h. The CHO-K1 cells expressing H2B-GFP were single clones co-transfected with pBOS-H2B-GFP<sup>20</sup> (BD Biosciences, San Jose, CA, USA) and pPGK-puro<sup>2</sup> and established by selection with puromycin at a concentration of 10  $\mu\text{g}/\text{mL}$ . Time-lapse imaging was performed using the LCV110 imaging system (Olympus) with a 20 $\times$  or 80 $\times$  phase contrast objective lens at 3-min intervals, and the acquired images were analyzed with MetaMorph software.

#### Observation of microtubule formation during mitosis

The plasmid vector pEGFP-tub (Takara Bio, Clontech) encoding EGFP- $\alpha$ -tubulin was transfected into the CHO-K1 cells together with the pCMV-Bsd vector<sup>26</sup> (Thermo Fisher Scientific; Waltham, MA, USA) to generate EGFP- $\alpha$ -tubulin-expressing CHO cells, which were enriched by drug selection with 8  $\mu\text{g}/\text{mL}$  blasticidin S. Then, the transfected CHO cells were treated with the indicated drugs for 6 h, fixed with 4% paraformaldehyde, and analyzed using an LSM 780 confocal microscope system. The captured images were analyzed with the attached ZEN 2010 imaging software (Carl Zeiss).

#### Assessment of MMCT efficiency

Microcells were prepared from one T-25 flask cultured with CHO cells and used for microcell-fusion experiments with one 60-mm dish of HT1080 cells. Micronucleation was performed by treating the cells with colcemid or TR combinations for 48 h, which were then cultured with fresh medium for another 24 h. Micronucleation with TN-16 and griseofulvin was performed as previously described.<sup>14</sup> The recipient HT1080 cells ( $1 \times 10^6$  cells) were plated in 60-mm culture dishes (Thermo Fisher Scientific) the day before microcell fusion. For MMCT into human iPSCs, six T-25 flasks of the CHO cell line expressing AmV-fusogen were prepared, and one 60-mm culture dish containing  $1 \times 10^6$  human iPSCs was prepared for microcell-fusion experiments. To purify microcells, flasks were filled with medium containing 10  $\mu\text{g}/\text{mL}$  cytochalasin B (Merck Sigma-Aldrich) and centrifuged for 1 h at  $11,899 \times g$  using a JLA-10.500 rotor (Beckman; Brea, CA, USA). Pellets containing crude microcell preparations were resuspended in CHO culture medium and passed sequentially through membranes with 8-, 5-, and 3- $\mu\text{m}$  pore sizes (Whatman; Springfield Mill, UK). The collected microcells were used for cell fusion with recipient cells. The microcells prepared from CHO-21HAC2/MV,<sup>11</sup> CHO-MAC1/EcoV,<sup>13</sup> CHO-modified 21HAC2/AmV, and CHO-BHIG11/MV<sup>26</sup> cells were overlaid on the

recipient cells and co-cultured for 24 h. The fused cells were expanded in three 10-cm culture dishes (Thermo Fisher), and drug-resistant cells were selected with antibiotics for 14 days. HT1080 cells carrying 21HAC2 and BHIG11 were selected with 8  $\mu\text{g}/\text{mL}$  blasticidin S, and cells carrying MAC1 were selected with 800  $\mu\text{g}/\text{mL}$  G418. Human iPSCs carrying modified 21HAC2 were selected with 100  $\mu\text{g}/\text{mL}$  G418. Colonies of HT1080 cells were fixed in methanol, stained with 5% Giemsa, and counted to assess the efficiency of chromosome transfer. Colonies of human iPSCs were counted, and each colony was expanded for further analysis.

#### PCR analysis

Genomic DNA of drug-resistant cells was extracted using a Genra Puregene Cell Kit (Qiagen; Venlo, NL) following the manufacturer's instructions, and PCR was performed with KOD One PCR Master Mix following the manufacturer's instructions. The following PCR primers were used to detect each resistant gene on the HAC/MAC: bsd F (5'-CAACAGCATCCCCATCTCTG-3') and #21cen6R (5'-CCCGGCCAGATTTCAGATTTTATTAGGG-3') with a product of 3,641 bps for the detection of the blasticidin S-resistant gene on 21HAC2<sup>2</sup> (Figures S1A, S11A, and S11B), kj\_neo (5'-CATCGCCTTCTATCGCCTTCTTGACG-3') and m11\_7R (5'-CACTCTTTACCCTCCACCGCTAACCTTG-3') with a product of 6,630 bps for the detection of the neomycin resistant-gene on MAC1<sup>27</sup> (Figures S1B, S11C, and S11D), and EF1a Fw (5'-CACTGAGTGGGTGGAGACTG AAGTTAGG-3') and Neo817 (5'-GCAGCCGATTGTCTGTTGTG-3') with a product of 370 bps for the detection of the neomycin resistant-gene on modified 21HAC2<sup>6</sup> (Figures S1D and S11E). The PCR products were then resolved by electrophoresis on Agarose S gels (Fujifilm Wako) followed by staining with ethidium bromide (Fujifilm Wako). FastGene 1 kb DNA Ladder Plus (Nippon Genetics Co.; Tokyo, Japan) was used as a band size marker.

#### Chromosome Q-banding analysis and FISH

Chromosome spreads on glass slides were prepared as follows. HT1080 cells were treated with colcemid (0.1  $\mu\text{g}/\text{mL}$ ) for 1.5 h, NIH3T3 cells were cultured with colcemid (0.08  $\mu\text{g}/\text{mL}$ ) for 2 h, and human iPSCs were treated with Metaphase Arresting Solution (2  $\mu\text{g}/\text{mL}$  in culture medium) (Genial Helix; Chester, Cheshire, UK) and Chromosome Resolution Additive (Genial Helix) to induce metaphase arrest. After incubating for 1 h, the arrested cells were treated with 0.075 M KCl, fixed with a mixture of methanol and acetate (3:1), and spread on glass slides. Cells on the slides were stained with quinacrine mustard (Merck; Darmstadt, Germany) and Hoechst 33258 (Merck) to enumerate chromosomes. Images were captured with the Axio Imager Z2 fluorescence microscope and analyzed with ISIS or Ikaros software (Carl Zeiss). FISH analyses were performed on the prepared chromosome spreads using a digoxigenin-labeled alphoid DNA probe p11-4<sup>29</sup> to detect 21HAC2 and biotin-labeled targeted plasmid vector pVGNLH1<sup>27,30</sup> to detect MAC1. Digoxigenin-labeled probes were detected with rhodamine-conjugated anti-digoxigenin Fab fragments (Merck). The biotin-labeled probe was detected with fluorescein isothiocyanate-conjugated avidin (Merck). The biotin and digoxigenin labeling of DNA was performed

using a Nick Translation Mix (Roche; Basel, Switzerland). Chromosomal DNA was counterstained with DAPI. Images were captured using the Axio Imager Z2 fluorescence microscope and analyzed with ISIS software.

### Statistical analysis

Significant differences in MMCT efficiency and FISH analysis of chromosome maintenance were determined using the Student's *t* test. The Tukey-Kramer post-hoc test following one-way analysis of variance was used for the statistical analysis of the duration of meta-phase arrest. The Mann-Whitney *U*-test was used for the analysis of chromosome retention rates.

### DATA AND CODE AVAILABILITY

Supplemental movies described in the article are deposited and available at Mendeley Data at <https://data.mendeley.com/datasets/559bj6n8k/1> (<https://doi.org/10.17632/559bj6n8k.1>).

### SUPPLEMENTAL INFORMATION

Supplemental information can be found online at <https://doi.org/10.1016/j.omtn.2023.07.002>.

### ACKNOWLEDGMENTS

We thank Drs. H. Kugoh, M. Hiratsuka, and T. Ohira for critical discussions. This work was supported in part by Japan Society for the Promotion of Science (JSPS) KAKENHI grant numbers 18K15671 (N.U.), 15K19615 (N.U.), and 18H06005 (K.T.), Research Support Project for Life Science and Drug Discovery (BINDS) from Japan Agency for Medical Research and Development (AMED) under grant number JP22ama121046 (Y.K.), Centers for Clinical Application Research on Specific Disease/Organ (Type C) from AMED under grant number JP22bm1004001 (K.T. and Y.K.), AMED under grant number JP22gm1610006 (Y.K. and K.T.), Joint Research of the Exploratory Research Center on Life and Living Systems (ExCELLS) (ExCELLS program No. 21–101), and JST CREST grant number JPMJCR18S4, Japan (Y.K.). This research was partly performed at the Tottori Bio Frontier managed by Tottori Prefecture. We thank Susan Zunino, PhD, and J. Ludovic Croxford, PhD, from Edanz (<https://jp.edanz.com/ac>) for editing a draft of this manuscript.

### AUTHOR CONTRIBUTIONS

N.U., H.S., and H.M. conceived and designed the experiments. H.S. and K.H. performed TR treatment experiments with CHO-BHIG11 cells. N.U., H.M., K.H., K.Y., and T.M. performed chemical compound screening to induce micronuclei. H.M., K.H., and R.I. performed the live-cell imaging, evaluation of the MMCT, and FISH analyses of the obtained clones. T.S. produced the lentiviral vectors that expressed EcoV- and AmV-fusogens. N.U., H.S., S.H., H.M., T.K., M.O., and Y.K. wrote the manuscript.

### DECLARATION OF INTERESTS

M.O. is the CEO and a shareholder of *trans* Chromosomics Inc.

### REFERENCES

1. Fournier, R.E., and Ruddle, F.H. (1977). Microcell-mediated transfer of murine chromosomes into mouse, Chinese hamster, and human somatic cells. *Proc. Natl. Acad. Sci. USA* 74, 319–323.
2. Kazuki, Y., Hoshiya, H., Takiguchi, M., Abe, S., Iida, Y., Osaki, M., Katoh, M., Hiratsuka, M., Shirayoshi, Y., Hiramatsu, K., et al. (2011). Refined human artificial chromosome vectors for gene therapy and animal transgenesis. *Gene Ther.* 18, 384–393.
3. Oshimura, M., Uno, N., Kazuki, Y., Katoh, M., and Inoue, T. (2015). A pathway from chromosome transfer to engineering resulting in human and mouse artificial chromosomes for a variety of applications to bio-medical challenges. *Chromosome Res.* 23, 111–133.
4. Kouprina, N., Tomilin, A.N., Masumoto, H., Earnshaw, W.C., and Larionov, V. (2014). Human artificial chromosome-based gene delivery vectors for biomedicine and biotechnology. *Expet Opin. Drug Deliv.* 11, 517–535.
5. Moriwaki, T., Abe, S., Oshimura, M., and Kazuki, Y. (2020). Transchromosomal technology for genomically humanized animals. *Exp. Cell Res.* 390, 111914.
6. Kazuki, Y., Uno, N., Abe, S., Kajitani, N., Kazuki, K., Yakura, Y., Sawada, C., Takata, S., Sugawara, M., Nagashima, Y., et al. (2021). Engineering of human induced pluripotent stem cells via human artificial chromosome vectors for cell therapy and disease modeling. *Mol. Ther. Nucleic Acids* 23, 629–639.
7. Kazuki, Y., Gao, F.J., Li, Y., Moyer, A.J., Devenney, B., Hiramatsu, K., Miyagawa-Tomita, S., Abe, S., Kazuki, K., Kajitani, N., et al. (2020). A non-mosaic transchromosomal mouse model of down syndrome carrying the long arm of human chromosome 21. *Elife* 9, e56223.
8. Kazuki, Y., Akita, M., Kobayashi, K., Osaki, M., Satoh, D., Ohta, R., Abe, S., Takehara, S., Kazuki, K., Yamazaki, H., et al. (2016). Thalidomide-induced limb abnormalities in a humanized CYP3A mouse model. *Sci. Rep.* 6, 21419.
9. Tomizuka, K., Shinohara, T., Yoshida, H., Uejima, H., Ohguma, A., Tanaka, S., Sato, K., Oshimura, M., and Ishida, I. (2000). Double trans-chromosomal mice: maintenance of two individual human chromosome fragments containing Ig heavy and kappa loci and expression of fully human antibodies. *Proc. Natl. Acad. Sci. USA* 97, 722–727.
10. Satofuka, H., Abe, S., Moriwaki, T., Okada, A., Kazuki, K., Tanaka, H., Yamazaki, K., Hichiwa, G., Morimoto, K., Takayama, H., et al. (2022). Efficient human-like antibody repertoire and hybridoma production in trans-chromosomal mice carrying megabase-sized human immunoglobulin loci. *Nat. Commun.* 13, 1841.
11. Katoh, M., Kazuki, Y., Kazuki, K., Kajitani, N., Takiguchi, M., Nakayama, Y., Nakamura, T., and Oshimura, M. (2010). Exploitation of the interaction of measles virus fusogenic envelope proteins with the surface receptor CD46 on human cells for microcell-mediated chromosome transfer. *BMC Biotechnol.* 10, 37.
12. Uno, N., Uno, K., Zatti, S., Ueda, K., Hiratsuka, M., Katoh, M., and Oshimura, M. (2013). The transfer of human artificial chromosomes via cryopreserved microcells. *Cytotechnology* 65, 803–809.
13. Suzuki, T., Kazuki, Y., Oshimura, M., and Hara, T. (2016). Highly efficient transfer of chromosomes to a broad range of target cells using Chinese hamster ovary cells expressing murine leukemia virus-derived envelope proteins. *PLoS One* 11, e0157187.
14. Liskovych, M., Lee, N.C., Larionov, V., and Kouprina, N. (2016). Moving toward a higher efficiency of microcell-mediated chromosome transfer. *Mol. Ther. Methods Clin. Dev.* 3, 16043.
15. Suzuki, T., Kazuki, Y., Hara, T., and Oshimura, M. (2020). Current advances in microcell-mediated chromosome transfer technology and its applications. *Exp. Cell Res.* 390, 111915.
16. Paulis, M., Susani, L., Castelli, A., Suzuki, T., Hara, T., Straniero, L., Duga, S., Strina, D., Mantero, S., Caldana, E., et al. (2020). Chromosome transplantation: a possible approach to treat human X-linked disorders. *Mol. Ther. Methods Clin. Dev.* 17, 369–377.
17. Salmon, E.D., McKeel, M., and Hays, T. (1984). Rapid rate of tubulin dissociation from microtubules in the mitotic spindle in vivo measured by blocking polymerization with colchicine. *J. Cell Biol.* 99, 1066–1075.

18. Dorléans, A., Gigant, B., Ravelli, R.B.G., Mailliet, P., Mikol, V., and Knossow, M. (2009). Variations in the colchicine-binding domain provide insight into the structural switch of tubulin. *Proc. Natl. Acad. Sci. USA* *106*, 13775–13779.
19. Rathinasamy, K., Jindal, B., Asthana, J., Singh, P., Balaji, P.V., and Panda, D. (2010). Griseofulvin stabilizes microtubule dynamics, activates p53 and inhibits the proliferation of MCF-7 cells synergistically with vinblastine. *BMC Cancer* *10*, 213.
20. Nakayama, Y., Uno, N., Uno, K., Mizoguchi, Y., Komoto, S., Kazuki, Y., Nanba, E., Inoue, T., and Oshimura, M. (2015). Recurrent micronucleation through cell cycle progression in the presence of microtubule inhibitors. *Cell Struct. Funct.* *40*, 51–59.
21. Samwer, M., Schneider, M.W.G., Hoefler, R., Schmalhorst, P.S., Jude, J.G., Zuber, J., and Gerlich, D.W. (2017). DNA cross-bridging shapes a single nucleus from a set of mitotic chromosomes. *Cell* *170*, 956–972.e23.
22. Santaguida, S., Tighe, A., D'Alise, A.M., Taylor, S.S., and Musacchio, A. (2010). Dissecting the role of MPS1 in chromosome biorientation and the spindle checkpoint through the small molecule inhibitor reversine. *J. Cell Biol.* *190*, 73–87.
23. D'Alise, A.M., Amabile, G., Iovino, M., Di Giorgio, F.P., Bartiromo, M., Sessa, F., Villa, F., Musacchio, A., and Cortese, R. (2008). Reversine, a novel Aurora kinases inhibitor, inhibits colony formation of human acute myeloid leukemia cells. *Mol. Cancer Therapeut.* *7*, 1140–1149.
24. Takahashi, K., Tanabe, K., Ohnuki, M., Narita, M., Ichisaka, T., Tomoda, K., and Yamanaka, S. (2007). Induction of pluripotent stem cells from adult human fibroblasts by defined factors. *Cell* *131*, 861–872.
25. Sinenko, S.A., Skvortsova, E.V., Liskoviykh, M.A., Ponomartsev, S.V., Kuzmin, A.A., Khudiakov, A.A., Malashicheva, A.B., Alenina, N., Larionov, V., Kouprina, N., and Tomilin, A.N. (2018). Transfer of synthetic human chromosome into human induced pluripotent stem cells for biomedical applications. *Cells* *7*, 261.
26. Iida, Y., Kim, J.H., Kazuki, Y., Hoshiya, H., Takiguchi, M., Hayashi, M., Erliandri, L., Lee, H.S., Samoshkin, A., Masumoto, H., et al. (2010). Human artificial chromosome with a conditional centromere for gene delivery and gene expression. *DNA Res.* *17*, 293–301.
27. Takiguchi, M., Kazuki, Y., Hiramatsu, K., Abe, S., Iida, Y., Takehara, S., Nishida, T., Ohbayashi, T., Wakayama, T., and Oshimura, M. (2014). A novel and stable mouse artificial chromosome vector. *ACS Synth. Biol.* *3*, 903–914.
28. Kneissig, M., Keuper, K., de Pagter, M.S., van Roosmalen, M.J., Martin, J., Otto, H., Passerini, V., Campos Sparr, A., Renkens, I., Kropveld, F., et al. (2019). Micronuclei-based model system reveals functional consequences of chromothripsis in human cells. *Elife* *8*, e50292.
29. Ikeno, M., Masumoto, H., and Okazaki, T. (1994). Distribution of CENP-B boxes reflected in CREST centromere antigenic sites on long-range alpha-satellite DNA arrays of human chromosome 21. *Hum. Mol. Genet.* *3*, 1245–1257.
30. Abe, S., Honma, K., Okada, A., Kazuki, K., Tanaka, H., Endo, T., Morimoto, K., Moriwaki, T., Hamamichi, S., Nakayama, Y., et al. (2021). Construction of stable mouse artificial chromosome from native mouse chromosome 10 for generation of transchromosomal mice. *Sci. Rep.* *11*, 20050.
31. Hasegawa, Y., Ikeno, M., Suzuki, N., Nakayama, M., and Ohara, O. (2018). Improving the efficiency of gene insertion in a human artificial chromosome vector and its transfer in human-induced pluripotent stem cells. *Biol. Methods Protoc.* *3*, bpy013.
32. Uno, N., Takata, S., Komoto, S., Miyamoto, H., Nakayama, Y., Osaki, M., Mayuzumi, R., Miyazaki, N., Hando, C., Abe, S., et al. (2022). Panel of human cell lines with human/mouse artificial chromosomes. *Sci. Rep.* *12*, 3009.
33. Vcelar, S., Melcher, M., Auer, N., Hrdina, A., Puklowski, A., Leisch, F., Jadhav, V., Wenger, T., Baumann, M., and Borth, N. (2018). Changes in chromosome counts and patterns in CHO cell lines upon generation of recombinant cell lines and subcloning. *Biotechnol. J.* *13*, e1700495.
34. Verweij, J., Clavel, M., and Chevalier, B. (1994). Paclitaxel (Taxol) and docetaxel (Taxotere): not simply two of a kind. *Ann. Oncol.* *5*, 495–505.
35. Mattei, J.C., Bouvier-Labit, C., Baretts, D., Macagno, N., Chocry, M., Chibon, F., Morando, P., Rochwerger, R.A., Duffaud, F., Olschwang, S., et al. (2020). Pan Aurora Kinase Inhibitor: A promising targeted-therapy in dedifferentiated liposarcomas with differential efficiency depending on sarcoma molecular profile. *Cancers* *12*, 583.
36. Pitts, T.M., Bradshaw-Pierce, E.L., Bagby, S.M., Hyatt, S.L., Selby, H.M., Spreafico, A., Tentler, J.J., McPhillips, K., Klauck, P.J., Capasso, A., et al. (2016). Antitumor activity of the aurora a selective kinase inhibitor, alisertib, against preclinical models of colorectal cancer. *Oncotarget* *7*, 50290–50301.
37. Helfrich, B.A., Kim, J., Gao, D., Chan, D.C., Zhang, Z., Tan, A.C., and Bunn, P.A., Jr. (2016). Barasertib (AZD1152), a small molecule aurora B inhibitor, inhibits the growth of SCLC cell lines in vitro and in vivo. *Mol. Cancer Therapeut.* *15*, 2314–2322.
38. Mammel, A.E., Huang, H.Z., Gunn, A.L., Choo, E., and Hatch, E.M. (2022). Chromosome length and gene density contribute to micronuclear membrane stability. *Life Sci. Alliance* *5*, e202101210.
39. Miga, K.H., Koren, S., Rhie, A., Vollger, M.R., Gershman, A., Bzikadze, A., Brooks, S., Howe, E., Porubsky, D., Logsdon, G.A., et al. (2020). Telomere-to-telomere assembly of a complete human X chromosome. *Nature* *585*, 79–84.
40. Roukos, V., Voss, T.C., Schmidt, C.K., Lee, S., Wangsa, D., and Misteli, T. (2013). Spatial dynamics of chromosome translocations in living cells. *Science* *341*, 660–664.